Discrete-variational Dirac–Slater calculations on the valence band XPS for α-uranium metal

Masayoshi Kurihara [a,*], Masaru Hirata [b], Rika Sekine [c], Jun Onoe [d], Hirohide Nakamatsu [e]

[a] *Nikkankyo Co. Ltd., 3-992-11, Higashishikawa, Hitachinaka-shi, Ibaraki-ken 312-0052, Japan*
[b] *Department of Materials Science, Tokai Research Establishment, Japan Atomic Energy Research Institute, 2-4 Shirakata, Tokai-mura, Naka-gun, Ibaraki-ken 319-1195, Japan*
[c] *Department of Chemistry, Faculty of Science, Shizuoka University, 836 Ohya, Shizuoka 422-8529, Japan*
[d] *The Institute of Physical and Chemical Research (RIKEN), 2-1 Hirosawa, Wako, Saitama 351-0198, Japan*
[e] *Institute for Chemical Research, Kyoto University, Uji, Kyoto 611-0011, Japan*

Abstract

We have performed relativistic molecular orbital calculations for the valence band structure of α-uranium metal, using the discrete-variational Dirac–Slater (DV-DS) method. We have used a U_9 model cluster for the calculation of the bulk electronic structure of α-uranium metal. The calculated valence X-ray photoelectron spectrum (XPS) which is obtained from the U_9 model cluster agrees well with the experimental spectrum. The peaks in the experimental spectrum are assigned to atomic components on the basis of the partial density of states (pDOS) for uranium atomic orbitals (AOs). © 2000 Elsevier Science B.V. All rights reserved.

PACS: 71.15.Mb; 71.15.Rf; 71.24.+q; 73.20.At

1. Introduction

Uranium metal in α-phase has been studied not only for reactor fuel application but also for academic interests regarding magnetic structures and superconductivity. Although a large number of experiments on the physical properties of uranium metal have been made so far, a little is known about its electronic structure and related phenomena. For example, experimental X-ray photoelectron spectra (XPS) of α-uranium metal were reported in 1970s [1–7]; however, the experimental spectra have not been explained quantitatively yet.

Electronic structure calculations for α-uranium metal have been performed using full-potential band calculations [8], symmetrized relativistic APW [9–11] and relativistic LAPW [12] methods. Yamagami and Hasegawa

reported that U 5f atomic orbital (AO) forms a wide band which was mainly due to the hybridization with the U 6d AO and spread around the Fermi level (E_F) for 0.2 Ry [10,11]. Willis and Eriksson [8] pointed out that U 5f electrons participate in the chemical bonds. Yamagami and co-worker [10] and Freeman et al. [12] qualitatively explained the XPS spectrum [4] near E_F with the density of states (DOS) of U 5f components. The DOS of U 5f near E_F explained the XPS spectrum qualitatively. However, they did not discuss the other components contributing to the valence band region. The participation of U 6d and other components is important in understanding the XPS spectrum and the electronic structure.

Quantitative comparison of first-principles calculations with the XPS spectra reveals the contribution of the U 5f, U 6d and other electrons to the chemical bonding of uranium metal. It is well known that relativistic effects play a significant role in electronic structures and chemical bonding in compounds containing heavy elements such as uranium [13,14]. Recently, we

---

* Corresponding author.
E-mail address: msys.kurihara@nifty.ne.jp (M. Kurihara).

have applied the fully relativistic discrete-variational Dirac–Slater (DV-DS) MO method to the assignment of XPS for UF_6 [15,16], UF_4 [17], uranyl nitrate $UO_2(NO_3)_2 \cdot 2H_2O$ [18] and uranium monocarbide (UC) [19,20], and shown that the calculated peak energies and relative intensities are in good agreement with the experimental results.

The purpose of this paper is to assign the experimental XPS for α-uranium metal to the atomic components by the DV-DS method and to understand the electronic structure of α-phase uranium metal.

2. Model cluster and computational method

The one-electron DS Hamiltonian is written as

$$\mathbf{H} = c\alpha\mathbf{P} + \beta mc^2 + V(\mathbf{r}), \tag{1}$$

where c, $\mathbf{P}$, m, α, β and $V(\mathbf{r})$ denote the velocity of light, the operator of momentum, the rest mass of electron, the Dirac matrices and the sum of Coulomb and exchange potentials, respectively. The molecular wave functions were obtained by means of linear combinations of AOs which were calculated by numerically solving the atomic DS equations. In the DV-DS code called RSCAT used here [21,22], the AOs were numerical solutions for an atomic-like potential obtained at an initial stage of each iteration for the self-consistent procedure. The atomic-like potential for the basis set was derived from spherical average of the molecular charge density around each nucleus. One-center (atomic) charge distributions were estimated by means of the Mulliken population analysis [23–26] in the self-consistent charge (SCC) method [27] which was adopted to approximate the self-consistent field. The computational details of the DV-DS method have been described elsewhere [28].

Fig. 1 shows the structure of α-uranium metal where eight uranium atoms (2)–(8) surround the central atom (1). The unit cell has four U atoms inside. Corresponding to the arrangement of the atoms numbered in Fig. 1, the U_9 cluster shown in Fig. 2 was employed as a model cluster for α-uranium metal in the present work. The geometry of the cluster was assumed to be of C_{2v} symmetry with the U–U bond lengths of 5.219 a.u. for atoms (1)–(2), 5.389 a.u. for (1)–(4) and 6.165 a.u. for (1)–(6) and (1)–(8) on the basis of the crystal structure for α-uranium metal [29]. Symmetry orbitals for the irreducible representations of C_{2v} symmetry were constructed from the AOs by the projection operator method [30]. All the calculations were performed with the Slater exchange parameter α of 0.7. The DV sample points of 18,000 were used for the present calculation. The basis functions up to the 7p orbital were used for the uranium atom. The calculations were carried out self-consistently until the difference between the initial
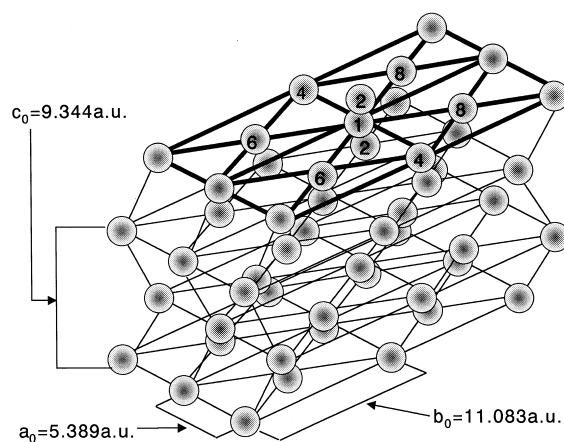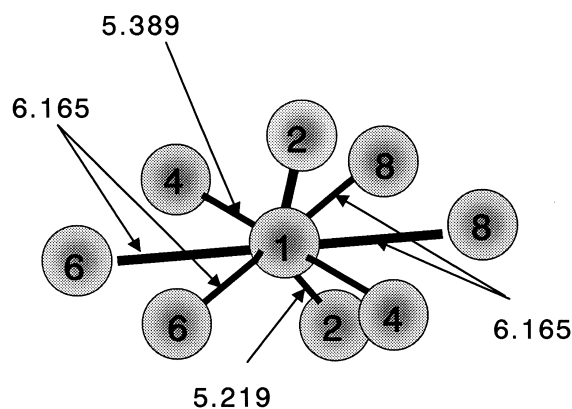

Fig. 1. Orthorhombic structure of α-uranium metal.

Fig. 2. U_9 model cluster of α-uranium metal. Bond lengths are in the atomic unit.

and final orbital populations in the iteration was less than 0.01.

The XPS intensity was estimated using the following equation proposed by Gelius [31]:

$$I_l \propto \sum_i \sigma_i P_{il}, \tag{2}$$

where I_l was the probability of photoionization from the lth MO level, σ_i the photoionization cross-section of the ith AO and P_{il} was the population of the ith AO in the lth MO. The photoionization cross-section values of U 5f to U 7s were taken from [32]. The cross-section of U 7p was ignored, because it was considered to be very small. For P_{il}, the gross population was evaluated by the Mulliken population analysis. Theoretical spectra were obtained by replacing each level with a Gaussian curve with a full width of half maximum (FWHM) of 1.6 eV.

Table 1
Valence levels, gross populations and XPS intensities for U_9 cluster of α-uranium metal

| Orbital | Energy (eV) | | Relative intensity | Gross orbital population of U | | | | | | |
	Ground state MO eigenvalue	Energy relative to HOMO		$5f_{5/2}$ (0.261)[a]	$5f_{7/2}$	$6p_{1/2}$ (0.085)	$6p_{3/2}$	$6d_{3/2}$ (0.042)	$6d_{5/2}$	$7s_{1/2}$ (0.01)
$417_{\gamma5}$	−2.69	+0.12	0.226	0.685	0.162			0.046	0.066	0.015
$416_{\gamma5}$	−2.72	+0.09	0.233	0.769	0.112			0.041	0.042	0.021
$415_{\gamma5}$[b]	−2.77	+0.04	0.234	0.746	0.136			0.035	0.051	0.017
$414_{\gamma5}$[c]	−2.81	0.00	0.224	0.722	0.112			0.031	0.062	0.044
$413_{\gamma5}$	−2.82	−0.01	0.220	0.697	0.124			0.044	0.098	0.015
$412_{\gamma5}$	−2.91	−0.10	0.200	0.554	0.173			0.078	0.149	0.024
$411_{\gamma5}$	−2.94	−0.13	0.208	0.615	0.155			0.063	0.097	0.032
$410_{\gamma5}$	−2.97	−0.16	0.209	0.609	0.169			0.046	0.070	0.063
$409_{\gamma5}$	−3.02	−0.21	0.198	0.542	0.189			0.045	0.103	0.066
$408_{\gamma5}$	−3.17	−0.36	0.181	0.440	0.199		0.008	0.110	0.202	0.013
$407_{\gamma5}$	−3.22	−0.41	0.162	0.395	0.176		0.005	0.061	0.204	0.105
$406_{\gamma5}$	−3.24	−0.43	0.167	0.411	0.171			0.099	0.224	0.047
$405_{\gamma5}$	−3.28	−0.47	0.166	0.391	0.197			0.167	0.113	0.078
$404_{\gamma5}$	−3.38	−0.57	0.159	0.388	0.169			0.139	0.172	0.076
$403_{\gamma5}$	−3.54	−0.73	0.142	0.298	0.177			0.204	0.197	0.091
$402_{\gamma5}$	−3.67	−0.87	0.135	0.262	0.170			0.227	0.305	0.008
$401_{\gamma5}$	−3.72	−0.91	0.134	0.255	0.179		0.008	0.197	0.264	0.061
$400_{\gamma5}$	−3.78	−0.97	0.136	0.265	0.170		0.005	0.240	0.290	0.040
$399_{\gamma5}$	−4.07	−1.26	0.102	0.170	0.116		0.016	0.230	0.353	0.087
$398_{\gamma5}$	−4.14	−1.33	0.082	0.109	0.121		0.009	0.139	0.305	0.184
$397_{\gamma5}$	−4.20	−1.39	0.071	0.112	0.080		0.010	0.148	0.265	0.262
$396_{\gamma5}$	−4.36	−1.55	0.066	0.101	0.069		0.005	0.206	0.215	0.263
$395_{\gamma5}$	−4.41	−1.60	0.063	0.079	0.085		0.009	0.185	0.176	0.394
$394_{\gamma5}$	−4.59	−1.78	0.109	0.168	0.156		0.005	0.258	0.299	0.083
$393_{\gamma5}$	−4.62	−1.81	0.100	0.148	0.121			0.312	0.391	0.009
$392_{\gamma5}$	−5.06	−2.25	0.097	0.113	0.142		0.021	0.268	0.403	0.038
$391_{\gamma5}$	−5.36	−2.55	0.075	0.094	0.090		0.010	0.243	0.328	0.224

MO										
$390_{\gamma5}$	−5.38	−2.57	0.082	0.096	0.092		0.011	0.266	0.475	0.076
$389_{\gamma5}$	−5.53	−2.72	0.078	0.091	0.081		0.013	0.354	0.398	0.022
$388_{\gamma5}$	−5.74	−2.93	0.035	0.028	0.031		0.026	0.096	0.132	0.653
$387_{\gamma5}$	−16.59	−13.78	0.082	0.005		0.026	0.902	0.007	0.005	0.021
$386_{\gamma5}$	−17.29	−14.48	0.085			0.020	0.956	0.009	0.006	0.008
$385_{\gamma5}$	−17.80	−14.99	0.084			0.005	0.963	0.010	0.006	0.005
$384_{\gamma5}$	−17.95	−15.14	0.082			0.017	0.930	0.016	0.016	0.011
$383_{\gamma5}$	−18.73	−15.92	0.085			0.006	0.985			
$382_{\gamma5}$	−18.92	−16.11	0.085				0.988	0.005		
$381_{\gamma5}$	−19.08	−16.27	0.085			0.008	0.981			
$380_{\gamma5}$	−19.28	−16.47	0.084				0.986			
$379_{\gamma5}$	−19.37	−16.56	0.085				0.988			
$378_{\gamma5}$	−19.56	−16.75	0.083			0.005	0.971		0.007	
$377_{\gamma5}$	−19.68	−16.87	0.085				0.975	0.008	0.007	
$376_{\gamma5}$	−19.78	−16.97	0.083				0.975	0.005	0.006	
$375_{\gamma5}$	−19.97	−17.16	0.084				0.980		0.005	
$374_{\gamma5}$	−20.14	−17.33	0.083			0.006	0.964	0.010	0.008	
$373_{\gamma5}$	−20.27	−17.46	0.085			0.004	0.969	0.009	0.009	
$372_{\gamma5}$	−20.79	−17.98	0.085			0.010	0.965	0.012	0.006	
$371_{\gamma5}$	−20.83	−18.02	0.083			0.011	0.941	0.016	0.009	
$370_{\gamma5}$	−21.05	−18.24	0.084			0.012	0.952	0.018	0.006	
$369_{\gamma5}$	−27.37	−24.56	0.084			0.963	0.029			
$368_{\gamma5}$	−27.69	−24.88	0.084			0.979	0.013			
$367_{\gamma5}$	−27.78	−24.97	0.084			0.947	0.041			
$366_{\gamma5}$	−27.88	−25.07	0.084			0.974	0.014		0.006	
$365_{\gamma5}$	−28.07	−25.26	0.084			0.971	0.016		0.005	
$364_{\gamma5}$	−28.36	−25.55	0.085			0.993	0.005			
$363_{\gamma5}$	−28.46	−25.65	0.085			0.987	0.008			
$362_{\gamma5}$	−28.69	−25.88	0.084			0.976	0.011		0.008	
$361_{\gamma5}$	−28.78	−25.97	0.084			0.984	0.008		0.005	

[a] Photoionization cross-section per electron for each atomic orbital (Al Kα) is shown in parentheses [31].
[b] Lowest unoccupied molecular orbital (LUMO).
[c] Highest occupied molecular orbital (HOMO).

3. Results and discussion

Table 1 shows the valence MO levels for the U_9 model cluster of α-uranium metal. The column I exhibits one electron energy and the column II shows the energy relative to highest occupied molecular orbital (HOMO). The occupied energy levels can be divided into three parts: the first part 'A' (0 to −3 eV in the column II); the second part 'B' (−13 to −18 eV in the column II); the third part 'C' (−24 to −26 eV in the column II). The U 5f and U 6d components contribute to the part A. The U 5f AOs are mainly located around E_F, while the U 6d AOs are widely distributed in the range from −0.10 to −2.93 eV. The U $6p_{3/2}$ and U $6p_{1/2}$ components appear in almost their purity in the peaks B and C, respectively. Theoretical XPS intensity is also shown in Table 1. The relative intensity of each level is similar to each other in the parts B and C. In contrast to them, the relative intensity in the part A varies from 0.035 to 0.224, depending on the components in each molecular orbital. This intensity modulation is dominated by the amount of the U 5f component of which photoionization cross-section is by far the greatest in Table 1.

Fig. 3 shows the experimental valence band XPS spectrum (Al Kα X-ray source) [2] and the theoretical spectra which were obtained with the U_9 cluster for α-uranium metal. The theoretical XPS is composed of three peaks, A, B and C. These peaks correspond to the three parts A, B and C in Table 1. The partial density of states (pDOS) of the orbital components for the U_9 model cluster is also shown in Fig. 3. The U 6p levels appear at the lower energies and these components split into two groups by the spin–orbit interaction. It is found in the pDOS plot that the peak B in the theoretical XPS originates mainly from the U $6p_{3/2}$ orbital. The U $6p_{3/2}$ components distribute from −16 to −22 eV. The peak C in the theoretical XPS is constructed from the U $6p_{1/2}$ orbital and resides from −26 to −30 eV.

The U $5f_{5/2,7/2}$, U $6d_{3/2,5/2}$, U $7s_{1/2}$ and U $7p_{1/2,3/2}$ components contribute to the peak A which lies at E_F. The U 5f component around E_F is much greater than the U 6d component. The components of U 7s, U 7p and U 6d make a band which is merged with the narrow U 5f band as shown in the inset of Fig. 3. It is remarkable that the U 7s components are split into two peaks. The contraction of U 7s orbital is caused by the relativistic stabilization of orbitals with low angular momentum. Consequently, U 7s is localized to some extent and does not form a wide band like the U 6d band. The U 6d and U 7s components are distributed in the deeper part which corresponds to the tail of peak A of the experimental XPS. Although the photoionization cross-sections of U 6d and U 7s are small, the intensity of the tail of the peak A is enhanced by mixing the U 5f components with them. On
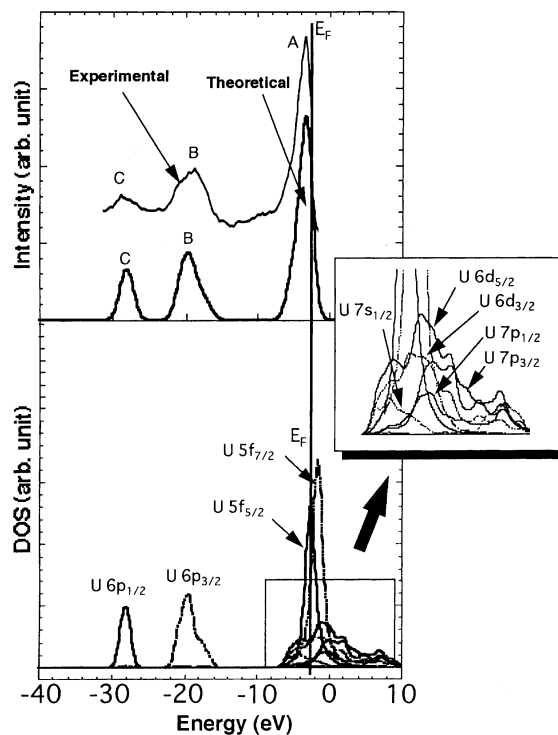

Fig. 3. Experimental [2], theoretical XPS and pDOS plots for U_9 model cluster of α-uranium metal.

the basis of the number of levels in each peak in Table 1, it is found that the total DOS for the peak A is 1.5 times larger than that for the peak B. The cross-section of photoionization of the U 5f electron is almost three times larger than that of U 6p. If the peak A would be composed of U 5f only, much higher peak A could appear than the actual peak A does. At last, well-estimated distributions of various orbital components provide a theoretical spectrum in good agreement with the experimental one. Therefore, it is concluded that the peak A includes significant contributions of other components in addition to U 5f, and the distributions of the U 6p, U 5f, U 6d, U 7s and U 7p components are successfully obtained in the present work.

In the previous band structure calculation [9], Yamagami and Hasegawa qualitatively derived the XPS spectrum of α-uranium metal. That is to say, the intensity of the XPS spectrum was not well described. In the present work, we have quantitatively obtained the valence XPS spectrum in the wide range and the intensity of each peak has been well reproduced by our theoretical method. We have confirmed the contribution of all valence electrons to the main peak A and clarified the valence band electronic structure of α-uranium metal.

4. Summary

We have applied the relativistic DV-DS MO method to obtain the theoretical valence band XPS spectrum of α-uranium metal, using the U_9 model cluster. We have obtained good agreement between the theoretical spectrum of the U_9 cluster and the experimental one for α-uranium metal in respect of both the peak positions and intensities. The peaks B and C are assigned to U $6p_{3/2}$ and U $6p_{1/2}$, respectively. The peak A at E_F is composed of U $5f$, U $6d$, U $7s$ and U $7p$ components.

Acknowledgements

References

[1] Karl-Christian, Buschbeck, Cornelius Keller (Eds.), Gmelin Handbook of Inorganic Chemistry, vol. A5 (Suppl. U Spectra), Springer, Berlin, 1982, p. 180.

[2] J.C. Fuggle, A.F. Burr, L.M. Watson, D.J. Fabian, W. Lang, J. Phys. F 4 (1974) 335.

[3] G.H. Lander, T.O. Brun, B.W. Veal, D.J. Lam, in: Proceedings of the First Conference on Crystalline Electric Field Effects in Metals and Alloys, University of Montreal, 1974, p. 480.

[4] B.W. Veal, D.J. Lam, Phys. Rev. B 10 (1974) 4902.

[5] Y. Bear, J.K. Lang, Phys. Rev. B 21 (1980) 2060.

[6] H. Grohs, H. Höchst, P. Steiner, S. Hüfner, Solid State Commun. 33 (1980) 573.

[7] G.C. Allen, I.R. Trickle, P.M. Tucker, Philos. Mag. B 43 (1981) 689.

[8] J.M. Willis, O. Eriksson, Phy. Rev. B 45 (1992) 13879.

[9] H. Yamagami, A. Hasegawa, J. Phys. Soc. Jpn. 59 (1990) 2426.

[10] A. Hasegawa, H. Yamagami, Prog. Theor. Phys. 108 (1992) 27.

[11] A.J. Freeman, D.D. Koelling, Physica B 86–88 (1977) 16.

[12] A.J. Freeman, D.D. Koelling, T.J. Watson-Yang, J. Phys. (Paris) C 4 (1979) 134.

[13] P. Pyykko, Adv. Quantum Chem. Rev. 11 (1978) 719.

[14] P. Pepper, B.E. Bursten, Chem. Rev. 91 (1991) 719.

[15] J. Onoe, K. Takeuchi, H. Nakamatsu, T. Mukoyama, R. Sekine, H. Adachi, J. Electron Spectrosc. Relat. Phenom. 60 (1992) 29.

[16] J. Onoe, K. Takeuchi, H. Nakamatsu, T. Mukoyama, R. Sekine, H. Adachi, J. Electron Spectrosc. Relat. Phenom. 70 (1994) 81.

[17] T. Mukoyama, H. Nakamatsu, H. Adachi, J. Electron Spectrosc. Relat. Phenom. 63 (1993) 409.

[18] M. Hirata, H. Monjyushiro, R. Sekine, J. Onoe, H. Nakamatsu, T. Mukoyama, H. Adachi, K. Takeuchi, J. Electron Spectrosc. Relat. Phenom. 83 (1997) 59.

[19] R. Sekine, H. Nakamatsu, T. Mukoyama, J. Onoe, M. Hirata, M. Kurihara, H. Adachi, Adv. Quantum Chem. 29 (1997) 123.

[20] M. Kurihara, M. Hitrata, R. Sekine, J. Onoe, H. Nakamatsu, T. Mukoyama, H. Adachi, J. Alloy Compounds 283 (1999) 128.

[21] H. Nakamatsu, H. Adachi, T. Mukoyama, Bull. Inst. Chem. Res. Kyoto Univ. 70 (1992) 16.

[22] J. Onoe, K. Takeuchi, H. Nakamatsu, T. Mukoyama, R. Sekine, B.-II Kim, H. Adachi, J. Chem. Phys. 99 (1993) 6810.

[23] R.S. Mulliken, J. Chem. Phys. 23 (1955) 1833.

[24] R.S. Mulliken, J. Chem. Phys. 23 (1955) 1841.

[25] R.S. Mulliken, J. Chem. Phys. 23 (1955) 2338.

[26] R.S. Mulliken, J. Chem. Phys. 23 (1955) 2343.

[27] A. Rosen, D.E. Ellis, H. Adachi, F.W. Averill, J. Chem. Phys. 65 (1976) 3626.

[28] A. Rosen, D.E. Ellis, J. Chem. Phys. 62 (1975) 3035.

[29] A.N. Holden, Physical Metallurgy of Uranium, Addison-Wesley, (1958) 27.

[30] J. Mayer, W.D. Sepp, B. Fricke, A. Rosen, Computer Phys. Commun. 54 (1989) 55.

[31] U. Gelius, J. Electron Spectrosc. Relat. Phenom. 5 (1974) 985.

[32] J.H. Scofield, J. Electron Spectrosc. Relat. Phenom. 8 (1974) 129.